ISSN 1063-7842, Technical Physics, 2018, Vol. 63, No. 2, pp. 216–219. © Pleiades Publishing, Ltd., 2018.
Original Russian Text © G.N. Churilov, N.S. Nikolaev, A.V. Cherepakhin, A.I. Dudnik, E.V. Tomashevich, M.V. Trenikhin, N.G. Bulina, 2018, published in Zhurnal Tekhnicheskoi Fiziki, 2018, Vol. 63, No. 2, pp. 224–227.

PHYSICAL SCIENCE OF MATERIALS

Thermal Oxidation of a Carbon Condensate Formed in High-Frequency Carbon and Carbon–Nickel Plasma Flow

G. N. Churilov[a,b,*], N. S. Nikolaev[a,b], A. V. Cherepakhin[b], A. I. Dudnik[a,b], E. V. Tomashevich[c], M. V. Trenikhin[d], and N. G. Bulina[e]

[a] *Kirensky Institute of Physics, Siberian Branch, Russian Academy of Sciences, Krasnoyarsk, 660036 Russia*

[b] *Siberian Federal University, Krasnoyarsk, 660041 Russia*

[c] *Institute of Chemistry and Chemical Technology, Siberian Branch, Russian Academy of Sciences, Krasnoyarsk, 660036 Russia*

[d] *Institute for Problems of Hydrocarbon Processing, Siberian Branch, Russian Academy of Sciences, Omsk, 644040 Russia*

[e] *Institute of Solid State Chemistry and Mechanochemistry, Siberian Branch, Russian Academy of Sciences, Novosibirsk, 630128 Russia*

**e-mail: churilov@iph.krasn.ru*

Received June 24, 2017

Abstract—We have reported on the comparative characteristics of thermal oxidation of a carbon condensate prepared by high-frequency arc evaporation of graphite rods and a rod with a hollow center filled with nickel powder. In the latter case, along with different forms of nanodisperse carbon, nickel particles with nickel core–carbon shell structures are formed. It has been found that the processes of the thermal oxidation of carbon condensates with and without nickel differ significantly. Nickel particles with the carbon shell exhibit catalytic properties with respect to the oxidation of nanosized carbon structures. A noticeable difference between the temperatures of the end of the oxidation process for various carbon nanoparticles and nickel particles with the carbon shell has been established. The study is aimed at investigations of the effect of nickel nanoparticles on the dynamics of carbon condensate oxidation upon heating in the argon–oxygen flow.

DOI: 10.1134/S1063784218020093

1. INTRODUCTION

It is well known that the processes of the oxidation of various carbon-based products are accelerated using metal catalysts. The high catalytic activity is intrinsic of 3*d* and platinum-group metals [1]. Pure metals and metals deposited onto carbon can be used [2]. During the plasma synthesis of various carbon-based nanostructures that use metals, metal core–carbon shell particles form along with fullerenes, nanotubes, graphenes, and amorphous carbon [3].

2. EXPERIMENTAL

Carbon condensate (CC) was synthesized in a high-frequency arc discharge facility in a helium atmosphere under normal pressure [4]. In the first case, annealed ultrahigh-purity graphite rods 6 mm in diameter were sputtered. In the second case, the sputtered rods had a hollow center filled with nickel (19% of the total sputtered mass). The prepared samples are referred to as CC1 and CC2, respectively. According to the X-ray diffraction data, sample CC1 contained fullerenes, graphite, and amorphous carbon phases and sample CC2 contained the same phases and the metallic nickel phase (Fig. 1).

Nickel–carbon plasma forms during the sputtering of graphite rods filled with nickel powder. After leaving the high-temperature discharge area, the plasma cools down and passes to the state of a homogeneous mixture of superheated nickel and graphite vapors. Nickel is almost insoluble in carbon; therefore, during the condensation of nickel and carbon vapors, carbon exudes on the surfaces of liquid nickel particles. Since nickel does not exist in the carbide (Ni_3C) state below 700°C, nickel core–carbon shell particles form upon cooling [4, 5].

It can be seen in Fig. 2 that the higher-contrast areas that correspond to nickel particles with pronounced layers are distributed directly in the amorphous carbon matrix. The nickel particle shell has a contrast that was analogous to that of the matrix, but is characterized by a noticeable layered structure.

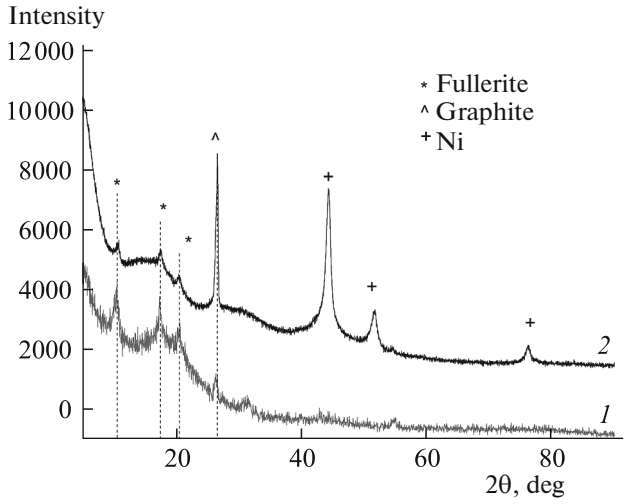

Fig. 1. X-ray diffraction patterns of (*1*) CC1 and (*2*) CC2 samples synthesized by sputtering graphite using high-frequency arc discharge. Patterns were obtained on a Bruker D8 Advance diffractometer.

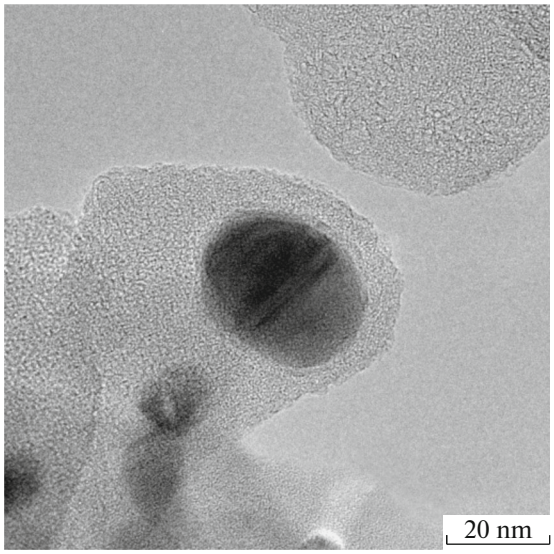

Fig. 2. TEM image of sample CC2 obtained on a Jeol JEM-2100 microscope at an accelerating voltage of 200 kV.

3. RESULTS AND DISCUSSION

The oxidation of samples CC1 and CC2 was studied by differential thermal analysis (DTA) and thermogravimetric analysis (TGA) using an NETZSCH STA 449 C Jupiter synchronous thermal analysis system. The samples were heated at a rate of 10°C/min in the Ar/O_2 (80%/20%) gas mixture flow.

The TGA data obtained on sample CC1 are presented in Fig. 3a. In the temperature range of 250–690°C, the exothermal reaction occurs. The temperature dependence of heat release is nonuniform and contains numerous peaks. The process is accompanied by significant mass loss (about 90%) in the sample. The most intense loss is observed in the temperature range of 390–620°C. This process corresponds to the burning of amorphous carbon and fullerenes, as well as other nanostructured forms of carbon [6].

The carbon condensate obtained by arc sputtering in the helium atmosphere has a soluble part presented by the fullerene mixture [6, 7].

The TGA data for the soluble part of sample CC1 are shown in Fig. 3b. It can be seen from the plot that, in the temperature range of 390–600°C, a reaction with the exothermal effect occurs. The sample loses 96% of its mass in the temperature range of 450–580°C. The temperature dependence of heat release contains one pronounced broadened peak. This peak broadens due to the difference between the reaction temperatures of different forms of fullerene with oxygen [8, 9].

Note that the burning enthalpies of sample CC1 and its soluble part are 17.4 and 19.3 kJ/g, respectively. This is indicative of the fact that the fullerene thermal oxidation reaction significantly contributes to the heat release during oxidation of the fullerene-containing CC.

The TGA data for sample CC2 are presented in Fig. 3c. The changes in sample CC2 are similar to those in sample CC1. However, it is worth noting that the exothermal peak in CC2 became more compact and less spread. The reaction with the heat release is observed in the temperature range of 280–536°C. The process occurs with the highest intensity and a mass loss of 62% in the range of 390–507°C. The oxidation enthalpy of sample CC2 is 14.9 kJ/g, which is somewhat lower than for CC1. This is related to the fact that the mass fraction of the fullerene mixture in sample CC2 is lower than in sample CC1 due to the presence of nickel.

In addition, samples CC1 and CC2 in the temperature ranges of 700–920°C and 620–850°C, respectively, exhibit another exothermal effect, which is also accompanied by mass loss. The mass loss is 8% and 5% for CC1 and CC2, respectively.

It is well known that the highly dispersed graphite reacts with oxygen at a temperature of about 700°C and carbon-based nanostructured products burn down at temperatures of 200–600°C [8, 9]. Taking this into account and relating the X-ray diffraction (XRD) and differential scanning calorimetry (DSC) data for samples CC1 and CC2, we may conclude that these samples contain graphite. This is confirmed by the fact that, upon the oxidation of the soluble part of CC1 without the graphite phase, the exothermal effect is the range of 650–1000°C is absent.

Sample CC2 was heated in a derivatograph under the same conditions. The heating was stopped at a temperature of 550°C and the sample was taken for investigations with X-ray photoelectron spectroscopy (XPS) and transmission electron microscopy (TEM).

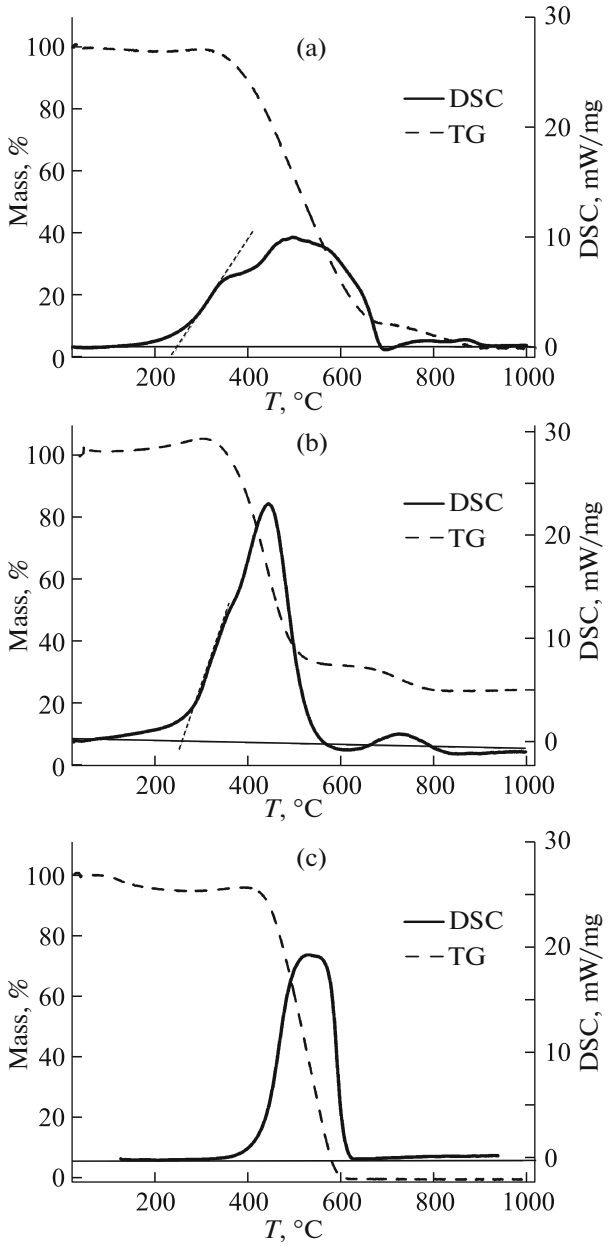

Fig. 3. Dependence of heat flow on temperature of heating in argon–oxygen gas mixture flow for (a) sample CC1, (b) soluble part of sample CC1, and (c) sample CC2.

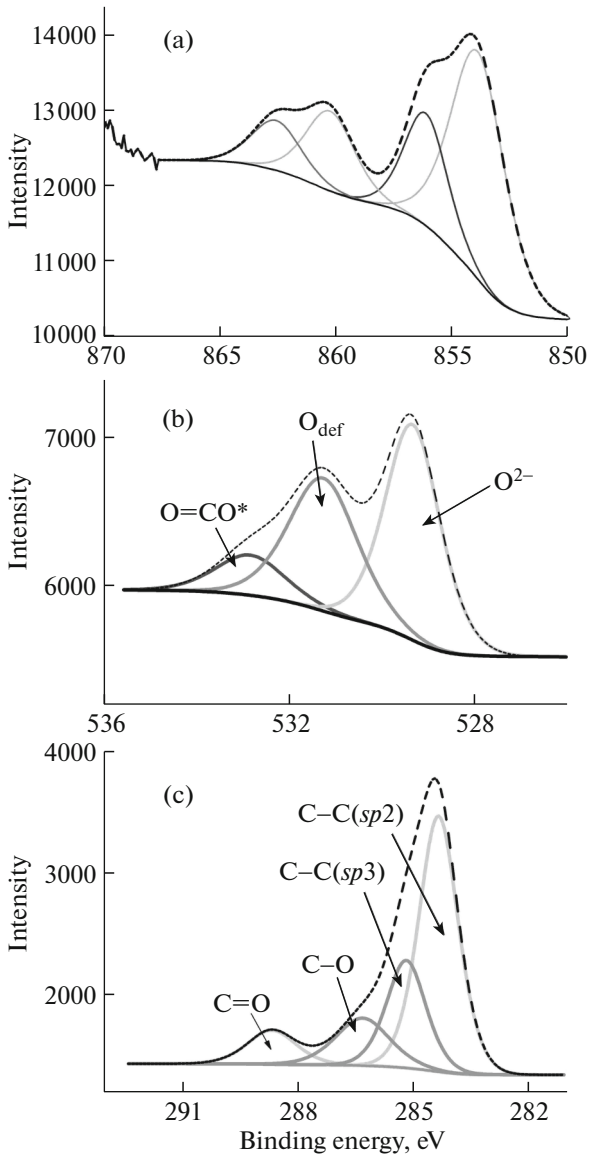

Fig. 4. XPS data for sample CC2 after heating to a temperature of 550°C in the argon–oxygen flow. (a) Ni 2*p* line in the range of 850–870 eV, (b) O 1*s* line in the range of 527–536 eV, and (c) line C 1*s* in the range of 281–293 eV.

The shape of nickel peaks (Fig. 4a) is almost identical to the shape characteristic of the NiO compounds [10–12] due to the large number of defects in the structure and the formation of insignificant amount of surface nickel hydroxide. In the O^{2-} peak oxygen spectra, there is the highest-intensity line with a binding energy of 529.3 eV, which corresponds to the NiO lattice. The line with a binding energy of about 531 eV corresponds to defect oxygen O_{def} (oxygen atom adjacent to Ni vacancies) and arises due to the large number of defects in the NiO structure [11]. In addition, upon the decomposition of the O 1*s* spectra, one can distinguish weaker lines with binding energies of 533.3 and 532.1 eV, which belong to the adsorbed water and oxygen-containing organic compounds on the surface. The main broad band, which has a binding energy in the carbon spectra, consists of contributions of graphite-like carbon with sp^2 hybridization (284.5 eV) and carbon with sp^3 hybridization (285.3 eV) (Fig. 4b). In addition, we can distinguish lines 286.3 and 288.6 eV, which can be attributed to the alcohol and carboxyl groups, respectively. Ion etching leads to a certain increase in the sp^3 hybridization fraction due to the disordering of graphite-like layers.

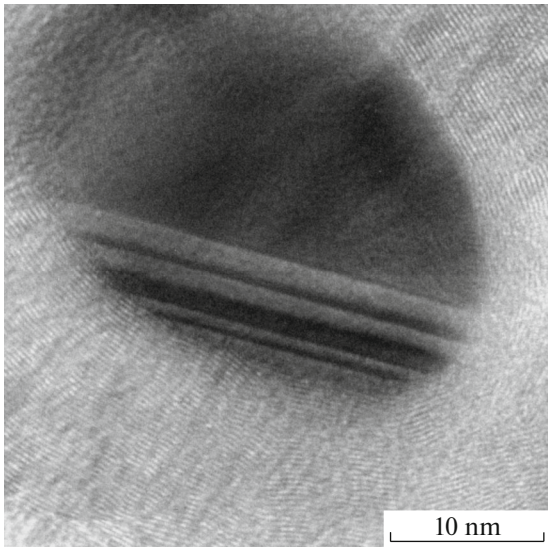

Fig. 5. TEM image of CC2 sample after heating obtained on a JEOL JEM-2100 microscope at an accelerating voltage of 200 kV.

According to the TEM data, CC2 sample after heating in the argon-oxygen mixture flow under the above-described conditions contains particles coated with the carbon shell (Fig. 5).

Based on the XPS and electron microscopy data, we may conclude that the CC obtained in the high-frequency plasma contains nickel-based core–shell particles. The particle core is polycrystalline nickel and the shell is carbon with the sp^3 hybridization near the nickel core, which transforms to carbon with the sp^2 hybridization on the outer particle shell boundary. Upon heating in the presence of oxygen, the nickel core is oxidized; the carbon shell is retained up to a temperature of 600°C. As the temperature further increases, the carbon shell burns out and retains a core that consists of polycrystalline nickel oxide nanoparticles.

4. CONCLUSIONS

It has been shown that all of the phases contained in CC1 formed by the arc sputtering of graphite rods, i.e., by fullerene synthesis in the oxygen–argon gas mixture flow, burn down, but at different temperatures of the burning maxima. The processes of burning different phases are superimposed, which allows us to conclude the impossibility of extracting any carbon phase by thermal oxidation in the oxygen flow. The introduction of nickel during sputtering leads to the occurrence of particles with the carbon shell–nickel core structure. Sample CC2, which contains these particles interacts more intensively with oxygen, and the highest-intensity process of burning all the phases shifts towards lower temperatures. The nickel particle cores were oxidized by heating sample CC2 to a temperature of 550°C in the presence of oxygen, yet the carbon shell remains stable. The carbon shell of nickel particles only burns down in the oxygen–argon mixture flow in the temperature range of 660–920°C. Specifically, there is the temperature region where stopping the oxygen supply can cause the carbon shell of particles burning down. Thus, thermal oxidation allows the nickel oxide core–carbon shell particles to be extracted from the CC synthesized with introduction of nickel.

ACKNOWLEDGMENTS

Transmission electron microscopy investigations were carried out on equipment of the Omsk Regional Center of Collective Use of the Siberian Branch of the Russian Academy of Sciences. This study was supported by the Russian Foundation for Basic Research, Government of Krasnoyarsk Territory, and the Krasnoyarsk Territorial Foundation for the Support of Scientific and R&D Activities, project no. 16-43-242148.

REFERENCES

1. P. S. Belov, I. A. Golubeva, and S. A. Nizova, *Ecology of the Production of Chemicals from Oil and Gas Hydrocarbons* (Khimiya, Moscow, 1991).
2. *Catalyst Technology*, Ed. by I. P. Mukhlenov (Khimiya, Leningrad, 1989).
3. E. A. Petrakovskaya, N. V. Bulina, G. N. Churilov, and A. P. Puzyr', Tech. Phys. **46**, 42 (2001).
4. N. V. Bulina, V. A. Lopatin, N. G. Vnukova, I. V. Osipova, and G. N. Churilov, Fullerenes, Nanotubes, Carbon Nanostruct. **15**, 395 (2007).
5. N. P. Lyakishev, *State Diagrams of Binary Metallic Systems* (Mashinostroenie, Moscow, 1996).
6. G. N. Churilov, A. Ya. Korets, and Ya. N. Titarenko, Zh. Tekh. Fiz. **66**, 191 (1996).
7. G. N. Churilov, O. A. Bayukov, E. A. Petrakovskaya, A. Ya. Korets, V. G. Isakova, and Ya. N. Titarenko, Tech. Phys. **42**, 1111 (1997).
8. H. S. Chen, A. R. Kortan, R. C. Haddon, and D. A. Fleming, J. Phys. Chem. **96**, 1016 (1992).
9. Y.-C. Hsieh, Y.-C. Chou, C.-P. Lin, T.-F. Hsieh, and C.-M. Shu, Aerosol Air Qual. Res. **10**, 212 (2010).
10. M. C. Biesinger, B. P. Payne, L. W. M. Lau, A. Gerson, and R. St. C. Smart, Surf. Interface Anal. **41**, 324 (2009).
11. M. C. Biesinger, B. P. Payne, A. P. Grosvenor, L. W. Lau, L. A. R. Gerson, and R. St. C. Smart, Appl. Surf. Sci. **257**, 2717 (2011).
12. B. P. Payne, M. C. Biesinger, and N. S. McIntyre, J. Electron Spectrosc. Relat. Phenom. **185**, 159 (2012).

Translated by E. Bondareva